

# Multichannel Dynamic Interfacial Printing: An Alternative Multicomponent Droplet Generation Technique for Lab in a Drop

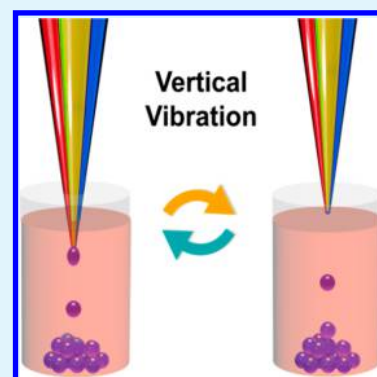
Shenglong Liao,<sup>†</sup> Xinglei Tao,<sup>†</sup> Yingjiao Ju,<sup>‡</sup> Jie Feng,<sup>\*,‡</sup> Wenbin Du,<sup>\*,‡</sup> and Yapei Wang<sup>\*,‡</sup>

<sup>†</sup>Department of Chemistry, Renmin University of China, Beijing 100872, China

<sup>‡</sup>State Key Laboratory of Microbial Resources, Institute of Microbiology, Chinese Academy of Sciences, Beijing 100101, China

**ABSTRACT:** Generation of uniform emulsion droplets mixed with multiple components is one of the key issues in the field of lab in a drop. Traditionally, droplet microfluidic chips are often served as the prime choice while designing and fabricating microfluidic chips always rely on skilled technician and specialized equipment, severely restricting its wide accessibility. In this work, an alternative technique, called multichannel dynamic interfacial printing (MC-DIP), was proposed for multicomponent droplet generation. The MC-DIP device was designed modularly and could be set up manually without any microfabrication process, exhibiting full accessibility for freshmen after a brief training. This new technique owns advantages in the generation of droplets with predictable sizes and composites. Quantitative experiments of measuring minimum inhibitory concentration (MIC) value via mixing microbes and antibiotics into droplet were conducted to proving its application potential for lab in a drop. Further research on a clinical pathogenic strain revealed that this technique could be potentially applied in the clinical laboratory for antibiotic susceptibility testing.

**KEYWORDS:** droplet generation, multicomponent, liquid mixing, MIC testing



## INTRODUCTION

Uniform emulsion droplets, as well as individual liquid cells, have attracted enormous research interests in fields of microreactor,<sup>1–7</sup> high throughput screening,<sup>8–10</sup> and biochemistry analysis<sup>11–15</sup> due to the ultrasmall amount of sample usage and remarkable repeatability for mimicking macroscale experiments. Based on the uniform emulsion droplets, lab in a drop,<sup>16,17</sup> as an emerging research field that means serving a drop as an individual laboratory, is developing rapidly. One of the fundamental yet essential issues for lab in a drop is the droplet generation technique. To guarantee the repeatability of lab in a drop, the required droplet generation technique should meet the basic demands of precise control over droplet size and droplet components. Besides considering the needs of researchers without any expertise in droplet generation, handling, and analysis, wide accessibility is another important concern that must be taken into account. Hence, developing a modular, easy-to-use, and stable droplet generation platform that meets the research requirements of users at different levels is of great importance for the booming development of lab in a drop.

Owing to the outstanding performance in controllable and precise liquid mixing and ultrasmall volume liquid handling, droplet microfluidic techniques were usually served as the prime choice for lab in a drop. Typically, droplet microfluidics are divided into three types including flow focusing,<sup>18–21</sup> T junction,<sup>22,23</sup> and coflow.<sup>24–26</sup> Designing and fabricating these microfluidic devices require skilled technicians and specialized equipment, sometimes restricting its expeditious practical application in laboratories without related experiences. Besides,

the droplet size is affected by many factors such as viscosity of fluid, interfacial tension, channel size, and so forth.<sup>27</sup> Thus, precise control of droplet size on a wide range is another challenge for entry-level users. How to reduce the technical threshold and increase the accessibility of droplet microfluidic techniques are being critical challenges for microfluidic researchers.<sup>28,29</sup> Great efforts have been devoted to putting the academic droplet microfluidic systems into commercial industry by simplifying and integrating microfluidic systems via modular design<sup>30–35</sup> or 3D printing of microfluidic chips.<sup>36,37</sup> However, the accessibility problem has not been solved completely since the revisions were still based on the modification of three basic droplet microfluidic methods and chips. Hence, new alternative droplet generation techniques are desirable to meet the general requirements of users at different levels.

Recently, we have proposed a simple active droplet generation technique<sup>38–40</sup> via the dynamic interfacial shearing driven by a mechanical device. However, the technique could only support one premixed solution that severely restricts the expansibility. Herein, upgraded from the previous study, we developed a new multicomponent active droplet generation technique called multichannel dynamic interfacial printing (MC-DIP). The newly developed technique converges multiple liquid components on the nozzle and generates droplets via the interfacial shearing due to the vibration of a multichannel

**Received:** October 30, 2017

**Accepted:** November 24, 2017

**Published:** November 24, 2017

capillary. The MC-DIP method can precisely generate droplets with controllable size and components like traditional droplet microfluidic methods. Compared with droplet microfluidic, the MC-DIP device composed of simple parts could be modularly assembled in several minutes without any complicated microfabrication. Therefore, the MC-DIP technique could perfectly meet the urgent demands of a widely accessible droplet generation technique for lab in a drop.

## EXPERIMENTAL SECTION

**Chemicals and the Device Setup.** The oil phase is composed of mineral oil (Sigma-Aldrich, St. Louis, MO) and *n*-tetradecane (TCI, Beijing, China) at a ratio of 1:1 (v/v), containing surfactants including 3 wt % ABIL EM 90 (Evonik Industries, Essen, Germany) and loaded in 96-well plates. A multibarrel (2, 3, or 7) glass capillary (World Precision Instruments Inc., Sarasota, FL) was heated with a blast burner and stretched into a tapered shape with a tip diameter of about 100–400  $\mu\text{m}$ . Each channel was connected with Teflon tubing and sealed with epoxy resin. The capillary was then hung on the cantilever of an electric vibrator, which was driven by a function generator. Syringes (100 or 250  $\mu\text{L}$ , Gastight, Hamilton Co., Reno, NV) were connected with Teflon tubing and set on several individual syringe pumps (Pump 11, PicoPlus Elite, Harvard Apparatus, Holliston, MA). After loading aqueous solutions in syringes, setting flow rates of different channels, and keeping the end of the multichannel capillary just below the oil surface, the MC-DIP process can begin with a steady vibration.

**Droplet Generation via the MC-DIP Method.** The multibarrel capillary includes 2C-capillary (two channels), 3C-capillary (three channels), and 7C-capillary (seven channels). Keeping flow rate of each channel at 1  $\mu\text{L}/\text{min}$  and setting the vibration frequency at 50 Hz, water droplets with different sizes were printed under the conditions of different numbers (*N*) of open channels. Conditions of *N* = 2 and *N* = 3 were set up with 2C-capillary and 3C-capillary, and 7C-capillary provided the conditions of *N* = 4–7. Droplet images were captured by an inverted fluorescence microscope (Eclipse Ti, Nikon, Tokyo, Japan), and the sizes were measured and analyzed with software (NIS-Elements, Nikon).

**Controlled Liquid Mixing with 3-Channel Capillary.** Taking 3C-capillary as a typical example, potassium hydrogen phthalate (KHP) buffer solutions (pH = 9.18) dissolved with fluorescein sodium (10.00  $\mu\text{g}/\text{mL}$ ) was loaded in two channels, and pure KHP buffer solution was loaded in another channel. The total flow rate of three channels was set at 3.00  $\mu\text{L}/\text{min}$ , and the vibration frequency was 50 Hz. The flow rate of each fluorescein sodium channel was changed among several values (0.10, 0.20, 0.30, 0.40, 0.50, 0.75, and 1.00  $\mu\text{L}/\text{min}$ ). Droplets were photographed by an inverted fluorescence microscope, and the fluorescence intensities of droplets were analyzed with software (NIS-Elements, Nikon). As a supporting experiment, a group of fluorescein sodium buffer solutions with the same concentration gradient as droplets were tested on a fluorescence spectrometer (F-4600, Hitachi, Tokyo, Japan).

**Microscale Chemical Reactions in Droplets.** For the chromogenic microreaction, aqueous solutions of starch (5 mg/mL), potassium iodide (0.05 mol/L), and ferric chloride (0.01 mol/L) were loaded into three separate channels. The total flow rate of three channels was set as 6.00  $\mu\text{L}/\text{min}$ , and the flow rate of starch was set as 2  $\mu\text{L}/\text{min}$ . The flow rate of ferric chloride was tuned among 0, 0.25, 0.50, 1.00, and 2.00  $\mu\text{L}/\text{min}$ . Droplets were collected in Eppendorf tube and photographed with a digital single-lens reflex camera (Canon EOS 70D, Tokyo, Japan). Relative gray values of pictures were recorded via Adobe Photoshop. The other microreaction was conducted in droplets mixed with acrylamide (200 mg/mL), *N,N'*-methylenebis(acrylamide) (MBAA, 5 mg/mL), ammonium persulfate (4 mg/mL), and *N,N,N',N'*-tetramethylethylenediamine (TMEDA, 2 mg/mL). Fluorescein sodium was added at the same time for easier characterization. The mixed droplets printed in oil phase were allowed to polymerize for about 10 min and then washed with petroleum ether repeatedly to remove surfactants.

**MIC Testing via the MC-DIP Technique.** *Escherichia coli* ATCC 25922 and *Staphylococcus aureus* ATCC 27217 were chosen as two model bacteria for MIC testing. Taking *E. coli* ATCC 25922 as a typical example: First, *E. coli* ATCC 25922 was cultured in Luria–Bertani medium (LB) overnight at 37 °C with a steady shaking speed at 200 rpm. Then the suspension of bacteria was diluted into  $\sim 6 \times 10^7$  CFU/mL ( $\text{OD}_{600} = 0.09$ ). Subsequently, the *E. coli* suspension was loaded in one channel, and the other two channels were loaded with pure Mueller–Hinton Broth (MHB) and MHB containing tetracycline hydrochloride salt (7.50  $\mu\text{g}/\text{mL}$ ). To generate droplets with volume of 1.00 nL and load each droplet with 10 bacteria on average, flow rate of the bacteria channel was set at 0.50  $\mu\text{L}/\text{min}$ . The flow rate of antibiotic channel ranged from 0 to 2.00  $\mu\text{L}/\text{min}$  with an interval of 0.20  $\mu\text{L}/\text{min}$ , and the MHB channel is tuned to keep the total flow rate at 3.00  $\mu\text{L}/\text{min}$ . About 2000 droplets were printed in each well by controlling the printing time at 40 s.

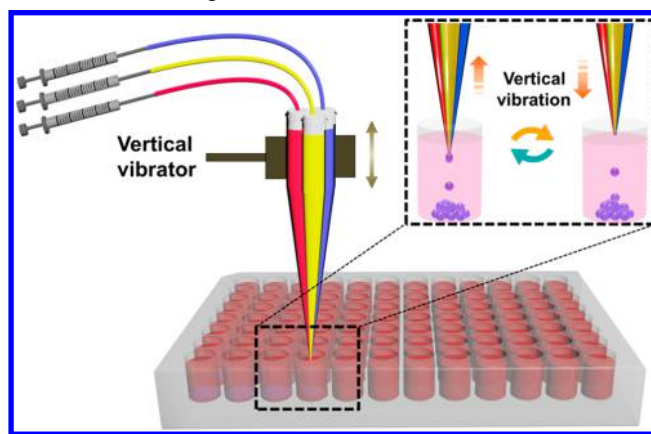
After cultured at 37 °C for 24 h, the droplets loading bacteria and antibiotics were photographed by an inverted microscope (Eclipse Ti, Nikon, Tokyo, Japan). Then these pictures were analyzed with ImageJ software. According to the surface roughness and turbidity, droplets with and without bacteria growth could be clarified and the bacteria growth percentage could be calculated.

Later, a clinical pathogenic strain of *Klebsiella pneumoniae* HS 11286 was selected for MIC testing. The operation process is the same with the procedure as stated above.

## RESULTS AND DISCUSSION

Typically, as illustrated in Scheme 1, a tapered 3-channel capillary connected with three syringes loading different

Scheme 1. Schematic Illustration of Multichannel Dynamic Interfacial Printing (MC-DIP)



components is allowed to vibrate at the oil surface. Because of the interfacial shearing process, the droplets mixed with three distinct components are “printed” into 96-well plate. Droplet components can be precisely controlled by tuning flow rate of discrete channels. To vividly present the advances of this technique in multicomponents mixing, three basic commercial inks were selected as three different components for MC-DIP. As shown in Figure 1a, by mixing three basic inks programmatically, various colorful droplets were printed into a 1.5 mL Eppendorf tube, indicating that MC-DIP is a potential platform for the preparation of droplets mixed with different components from different channels. Another qualitative experiment was conducted by mixing fluorescein sodium with acidic or basic solution into droplets via MC-DIP. As a pH-sensitive fluorescence dye, its fluorescence intensity increases as the increase of pH value.<sup>41</sup> As shown in Figure 1b, the carboxyl group of fluorescein sodium is protonated and tends to

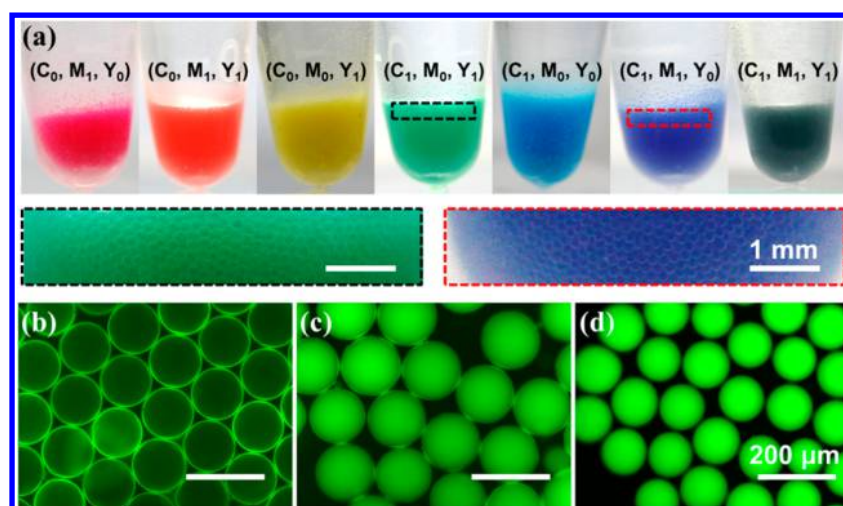


**Figure 1.** (a) Optical images of colorful droplets via controllable mixing of multiple inks. C: cyan; M: magenta; Y: yellow. The coordinate of  $(C_x, M_y, Y_z)$  means the flow rate of each ink in units of  $\mu\text{L}/\text{min}$ . Fluorescence images of acidic (b), neutral (c), and basic (d) droplets loading the same amount of fluorescein sodium.

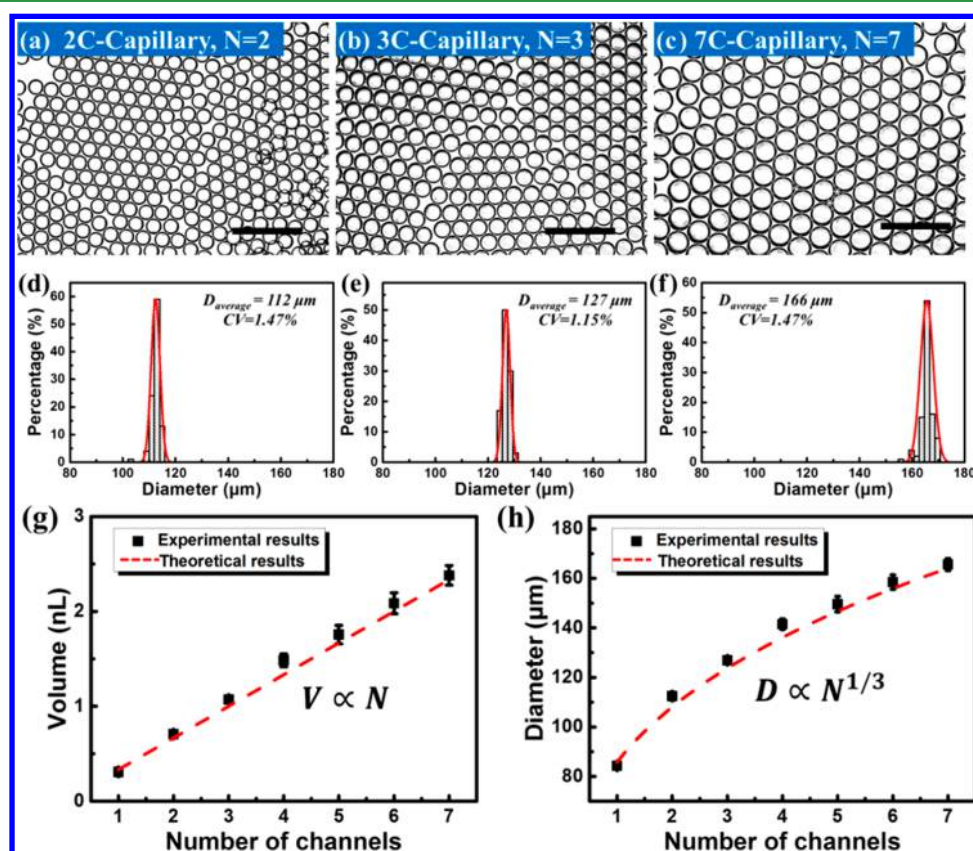


**Figure 2.** Droplet size controlled by the number of open channels with same flow rate in each channel ( $1.00 \mu\text{L}/\text{min}$ ). Optical images (a–c) and size distribution (d–f) of droplets generated with different numbers of open channels. Scale bar:  $500 \mu\text{m}$ . (g, h) The relationship between droplet size and the number of open channels. Droplet volume (g) and droplet diameter (h) versus the number of open channels.

precipitate in acidic conditions. Hence, it aggregates at the oil–water interface and the droplet fluorescence is weak. As the pH is increased and the carboxyl group is deprotonated, the fluorescence of droplets becomes brighter (Figure 1c,d).

As a candidate for the controllable multicomponent droplet generation technique, it is necessary to investigate MC-DIP for controlling the droplet size and components concentration. Prior to the controllable droplet components, the droplet size should be controlled and fixed first, ensuring the change in

concentration independent of droplet size. As previously reported, the single-channel DIP technique, the fact that the droplet size is mainly relevant to flow rate, and the vibration frequency have been revealed by the exhaustive principal study, which is believed to have the same influence on the MC-DIP. However, since the single channel is upgraded into multiple channels, further evaluation on the relationship between droplet size and channel number is necessary for MC-DIP. As noted in the single-channel DIP technique, only one droplet



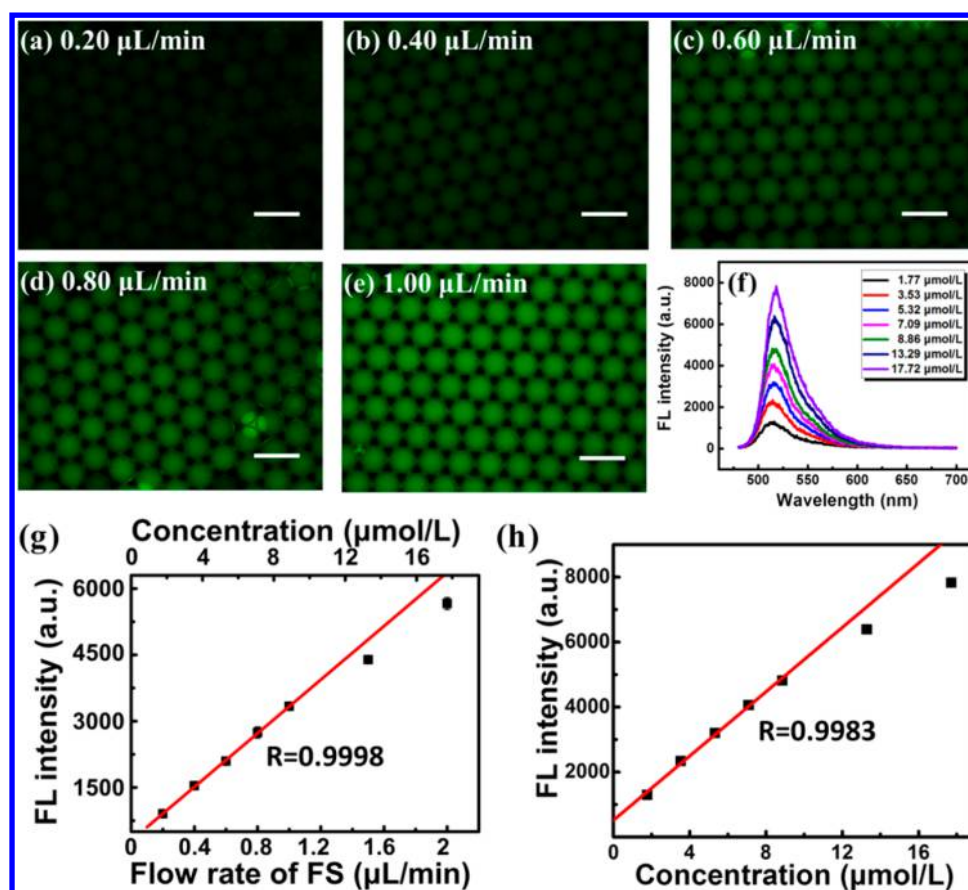


**Figure 3.** Quantitatively loading fluorescent dye into droplets. (a–e) Fluorescence images of droplets generated at different total flow rates of fluorescein sodium solution. Scale bar: 200 μm. (f) Fluorescent spectrum of fluorescein sodium solution with different concentrations. (g) Droplet fluorescent intensities under different flow rates of fluorescein sodium solution. (h) Fluorescent intensity of fluorescein sodium solution at different concentrations. Red line in (g, h): linear fitting curve of five points at low concentrations within which self-quenching is negligible.

was generated by the interfacial shearing for each vibration period during a typical printing process. Thus, the droplet volume is equal to the flow rate ( $Q$ ) divided by the vibration frequency ( $f$ ). In the MC-DIP process, liquids injected from different channels converge and mix into a droplet once they meet at the capillary tip. In this regard, it is reasonable to predict that the droplet volume should be a result of the total flow rate ( $\sum_{i=1}^N Q_i$ ) divided by the vibration frequency, as referred to in eq 1.

$$V = \frac{\sum_{i=1}^N Q_i}{f} \quad (1)$$

According to eq 2, the diameter of droplets ( $D$ ) can be then specified as

$$D = \left( \frac{6 \sum_{i=1}^N Q_i}{\pi f} \right)^{1/3} \quad (2)$$

To verify the accuracy of eq 1 as well as eq 2, water droplets were generated at different total flow rates by changing the number of open channels while the flow rates of each channel remain unchanged. As shown in Figure 2a–c, different kinds of capillary (2-, 3-, and 7-channel capillary) were chosen to conduct the experiments. When  $N$  varies from 2 to 7, the MC-DIP technique can successfully generate droplets with different sizes. It should be noted that all the droplets are highly uniform

and exhibit narrow size distribution regardless of the printing conditions (Figure 2d–f). In terms of the constant  $Q_i$ , the total flow rates are proportional to the channel number ( $N$ ). Theoretically, when changing the number of open channels, the droplet volume also exhibits a proportional relation to the number, which is consistent with the experimental results in Figure 2g. Accordingly, the diameters of droplets with the use of different channel numbers perfectly match with theoretical value (Figure 2h). According to the consistency between experimental results and theoretical value, it is convinced that liquids from every channel converge into a pendant drop, and the pendant drop is separated from the MC-DIP nozzle by interfacial shearing. The droplet size can be absolutely tuned by changing the channel flow rate and vibration frequency while it would be harder for common droplet microfluidics because droplet size generated via these methods exhibits relatively complicated relationship with channel size, liquid viscosity, and interfacial tension as well as flow rates. The simple droplet size model of MC-DIP is a remarkable advantage that can significantly reduce the difficulty of precisely generating uniform and multicomponent droplets for users without enough experience on droplet microfluidics. Thus, the MC-DIP technique could be served as an easy-operating and wide-accessible platform for multicomponent droplet generation.

After droplet size was well controlled, precisely tuning the droplet components should be quantitatively studied. As stated above, the droplet volume is proportional to the sum of flow

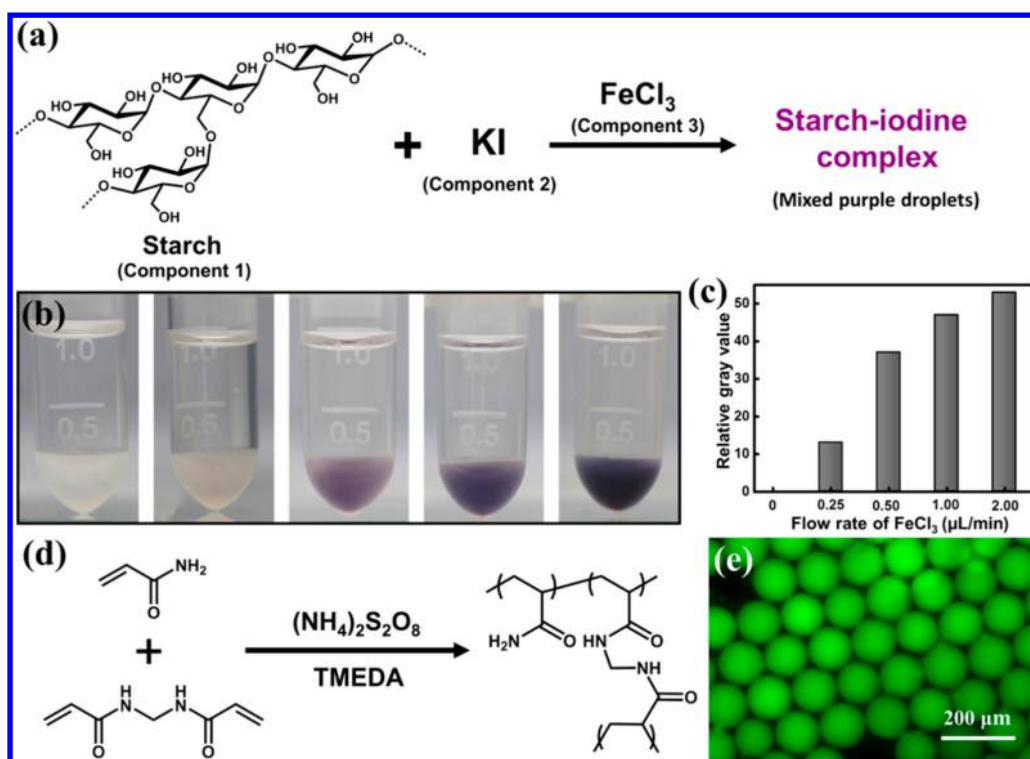


**Figure 4.** Microscale chemical reactions in droplets. (a) A three-component chromogenic reaction among starch, potassium iodide, and ferric chloride. (b) Optical images of three-component mixed droplets generated under different flow rates of ferric chloride. From left to right: 0.00, 0.25, 0.50, 1.00, and 2.00  $\mu\text{L}/\text{min}$ . (c) Relative gray value of pictures in (b). (d) The polymerization reaction of acrylamide in droplets. (e) Fluorescent image of polyacrylamide hydrogel microspheres dispersed in petroleum ether without surfactants.

rates. Thus, the concentration of one component in the droplet ( $c_{i,\text{droplet}}$ ) can be theoretically predicted according to eq 3:

$$c_{i,\text{droplet}} = \frac{c_{i,0}Q_i}{\sum_{i=1}^N Q_i} \quad (3)$$

where  $c_{i,0}$  is the concentration of one component in the mother solution. To identify this prediction, droplets loaded with quantitative fluorescent dye were printed via the MC-DIP. In the 3C-capillary which acts as the printing nozzle, one channel was loaded with potassium hydrogen phthalate (KHP) buffer solutions (pH = 9.18) and the other two were loaded with fluorescein sodium salt dissolved in the same buffer solution. As shown in Figure 3, keeping the total flow rate at 3.00  $\mu\text{L}/\text{min}$ , droplets loading fluorescein sodium were generated with the same volume but different amount of probing dyes by adjusting the flow rate of fluorescein sodium solution. According to the result analyzed by software in Figure 3g, the fluorescence intensity of these droplets is linearly proportional to the flow rate of fluorescein sodium, indicating that the concentration of fluorescein sodium can be precisely controlled in the droplets. When flow rates are tuned above 1.00  $\mu\text{L}/\text{min}$ , the fluorescence intensity shows deviation to the linear fitting curve, which should be attributed to the self-quenching caused by the molecular aggregation of fluorescein sodium at high concentrations. A similar trend was also observed in the bulk solutions, in which the fluorescence intensities are proportionally correlated with the dye concentration only at low concentration (Figure 3f,h). On the basis of the above results, it comes to a conclusion that MC-DIP can fully realize precise liquid mixing into droplets, holding great potential and promise for lab in a drop.

After confirming the precise control over droplet size and liquid mixing of MC-DIP, two kinds of model chemical reactions were miniaturized into tiny droplets via the MC-DIP method to demonstrate its application potential for microreactors. A simple chromogenic reaction was used for a vivid demonstration of microreactor application. As stated in Figure 4a, the mixture of starch and potassium iodide would become purple when it is encountered with ferric chloride. Therefore, three components were separately loaded into three channels and then mixed into droplets via the MC-DIP technique. The newly generated droplets quickly became purple. As the flow rate of ferric chloride increases, the droplet color tends to be deeper since an increasing amount of ferric chloride in droplets that can generate more triiodide ions (Figure 4b,c). Another model microreactor is the polymerization of acrylamide (Figure 4d) in the droplets mixed with monomer (acrylamide), cross-linker (MBAA), and initiators (ammonium persulfate and TMEDA). The emulsion droplets were always surrounded with surfactants for avoidance of droplet coalescence. After about 10 min for complete polymerization of acrylamide, the surfactants in oil phase were removed by petroleum ether. As shown in Figure 4e, droplet coalescence did not occur, indicating successful preparation of polyacrylamide hydrogel microspheres. The above two kinds of model microreactors based on the MC-DIP technique clearly demonstrated the potential of MC-DIP, suggesting that the MC-DIP technique is a reliable technique for chemical analysis or materials synthesis.

Taking advantage of precise liquid mixing into size controllable droplets, the MC-DIP technique was used to conduct a practical application to prove its full potential for lab in a drop. Traditionally, by mixing microbes and antibiotics in a tube or well plate, the minimum inhibitory concentration

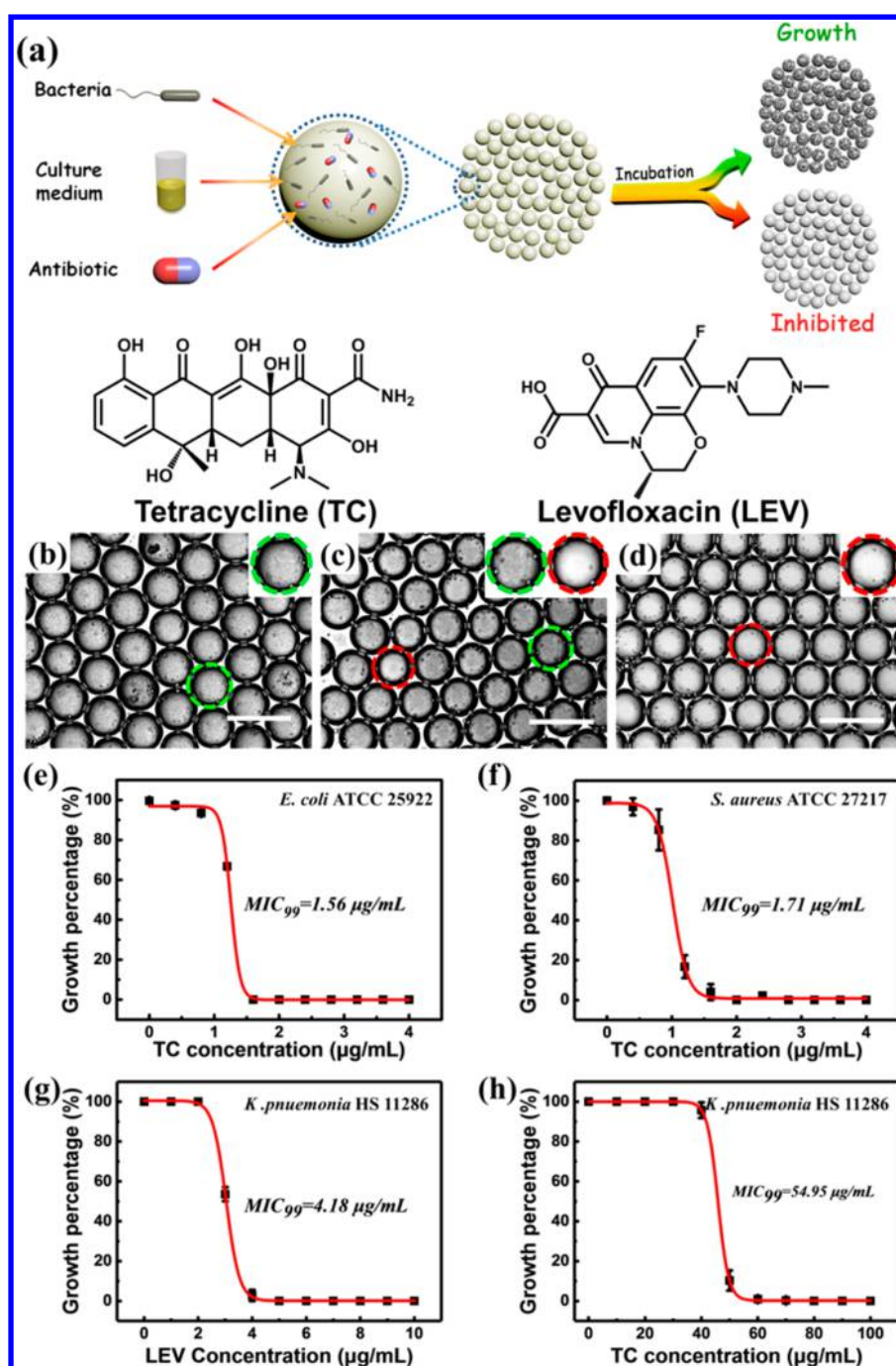


**Figure 5.** (a) Schematic illustration of MIC testing based on the MC-DIP technique and chemical structures of two antibiotics used in the following tests. (b–d) Optical images of droplets loaded with *E. coli* ATCC 25922 and different amount of antibiotic (tetracycline, TC). (b) 0  $\mu\text{g/mL}$ ; (c) 0.80  $\mu\text{g/mL}$ ; (d) 2.40  $\mu\text{g/mL}$ . Green dashed cycle: droplet with bacterial growth; red dashed cycle: droplet with inhibited or dead bacteria. Scale bar: 200  $\mu\text{m}$ . (e, f) Percentage of droplets with bacteria growth versus tetracycline concentration. (e) *E. coli* ATCC 25922; (f) *S. aureus* ATCC 27217. (g, h) Percentage of droplets with bacteria growth versus antibiotic concentration. (g) Levofloxacin; (h) tetracycline. The red curves in (e–h) are the fitting curves of all black points according to the DoseResp model.

(MIC) that always served as the gold standard for evaluating the bacterial inhibition effect of antibiotics could be measured based on liquid turbidity after incubation. The droplet method for MIC measurements has advantages of small amount of reagent consumption, large quantity of parallelization, and high sensitivity and thus attracted great interests in the field of lab in a drop.<sup>28,42,43</sup> Herein, the MC-DIP technique was used to generate droplets quantitatively mixed with microbes and antibiotics. After a certain time incubation, MIC could be read

out according to the turbidity of droplets with the help of a microscope. For example, two model microbes were selected for representative MIC measurements: a Gram-positive strain (*S. aureus* ATCC 27217) and a Gram-negative strain (*E. coli* ATCC 25922). To separate the bacteria with the antibiotic and keep an equal volume of each droplet, a typical 3C-capillary was selected for MIC testing. As shown in Figure 5a, bacteria suspension, antibiotic solution, and MH broth were separately loaded in three individual channels. By tuning the flow rate of



each channel, around 2000 droplets were printed in each well, with a constant 1 nL volume and bacteria concentration (about 10 cells per droplet), yet a gradient of antibiotic concentrations. After being incubated for 24 h at 37 °C, the plate was taken out for microscope inspection. As shown in Figure 5b, all of the droplets, loading *E. coli* ATCC 25922 without antibiotic, possess a rough droplet surface and appear dark gray with weak brightness due to the poor surface reflection, referring to a well-grown state of bacteria in the droplets (green dashed cycle). Loading the antibiotic of tetracycline in droplets up to a certain concentration, most droplets keep dark with a rough surface, while a few of them turn smooth with bright reflection on their surfaces (red dashed cycle, Figure 5c). These distinct droplets with a brighter and smoother surface refer to a state that bacterial growth is inhibited by tetracycline. When the concentration of tetracycline is increased, all droplets become bright and smooth (Figure 5d). On the basis of the bright-field images of replicated droplets with the same experimental condition in each well, we define the percentage of droplets with a dark and rough surface as the growth percentage, which represents the possibility of bacterial growth with a specific antibiotic concentration. Herein, the MIC value is defined as the concentration at which 99% of droplets become bright and clear, meaning 99% of possibility for successful bacterial inhibition at this concentration. As shown in Figures 5e and 5f, the MIC values of tetracycline to *E. coli* ATCC 25922 and *S. aureus* ATCC 27217 are 1.56 and 1.71  $\mu\text{g}/\text{mL}$ , respectively, consistent with MIC values determined via broth microdilution method (1 and 1  $\mu\text{g}/\text{mL}$ ). The good consistency with traditional gold methods convinces that this MC-DIP technique can be perfectly applied for droplet MIC testing. Moreover, compared with the common broth microdilution method based on 96-well plates which commonly repeats the tests only several times, the MIC determined via MC-DIP methods that are based on thousands of repeats tends to be more convincing for practical clinical diagnosis.

To further demonstrate the potential application in clinical diagnosis, the MC-DIP technique was applied to antibiotic susceptibility testing of a clinical multidrug-resistant strain of *K. pneumoniae* HS 11286 (separated from human sputum at Shanghai, China in 2011<sup>44</sup>). As shown in Figures 5g and 5h, the MIC values of levofloxacin and tetracycline determined by the MC-DIP method are 4.18 and 54.95  $\mu\text{g}/\text{mL}$ , also consistent with the results of the broth microdilution method (4 and 64  $\mu\text{g}/\text{mL}$ ). According to the Clinical & Laboratory Standards Institute (CLSI) criteria,<sup>45</sup> the MIC value of levofloxacin approximately equals to the intermediate criteria from CLSI (4  $\mu\text{g}/\text{mL}$ ), indicating *K. pneumoniae* HS 11286 is intermediate to levofloxacin. While the MIC result of tetracycline is much higher than the criteria of CLSI (8  $\mu\text{g}/\text{mL}$ ), indicating *K. pneumoniae* HS 11286 is resistant to tetracycline.

## CONCLUSION

In summary, we proposed a multichannel dynamic interfacial printing technique for controllable multicomponent droplet generation. The newly developed MC-DIP technique exhibits excellent performance in generating uniform droplets with predesigned size and components. Compared with traditional microfluidic devices, the MC-DIP devices are simply based on a cheap vibrator and handmade tapered multichannel capillary, which can be modularly assembled and used by freshmen after a brief training. To present its practical application, a series of droplets loading bacteria and antibiotics were generated via the

MC-DIP for MIC measurements, and the results match well with the classic broth microdilution method. In terms of great potential for further development, we believe it would become a promising tool for MIC testing in clinical laboratories or hospitals. In addition, as a promising technique for lab in a drop, the MC-DIP technique could also be used in the field of bioanalysis or microreactors. We have solid confidence that this new versatile technique is bound to be an important supplement to current chip-based droplet microfluidic techniques.

## AUTHOR INFORMATION

### Corresponding Authors

\*E-mail [fengj@im.ac.cn](mailto:fengj@im.ac.cn) (J.F.).

\*E-mail [wenbin@im.ac.cn](mailto:wenbin@im.ac.cn) (W.D.).

\*E-mail [yapeiwang@ruc.edu.cn](mailto:yapeiwang@ruc.edu.cn) (Y.W.).

### ORCID

Wenbin Du: 0000-0002-7401-1410

Yapei Wang: 0000-0001-5420-0364

### Notes

The authors declare no competing financial interest.

## ACKNOWLEDGMENTS

The authors thank Zhen Wang and Libing Dong for fluorescence measurement and preparation of bacterial samples. This work was financially supported by the National Natural Science Foundation of China (21674127, 21422407, 51373197, and 31470221), and Beijing Municipal Science & Technology Commission (Z161100000116042).

## REFERENCES

- (1) Elvira, K. S.; i Solvas, X. C.; Solvas, X.; Wootton, R. C.; deMello, A. J. The Past, Present and Potential for Microfluidic Reactor Technology in Chemical Synthesis. *Nat. Chem.* **2013**, *5*, 905–915.
- (2) Niu, G.; Ruditskiy, A.; Vara, M.; Xia, Y. Toward Continuous and Scalable Production of Colloidal Nanocrystals by Switching from Batch to Droplet Reactors. *Chem. Soc. Rev.* **2015**, *44*, 5806–5820.
- (3) Cui, J.; Zhu, W.; Gao, N.; Li, J.; Yang, H.; Jiang, Y.; Seidel, P.; Ravoo, B. J.; Li, G. Inverse Opal Spheres Based on Polyionic Liquids as Functional Microspheres with Tunable Optical Properties and Molecular Recognition Capabilities. *Angew. Chem., Int. Ed.* **2014**, *53*, 3844–3848.
- (4) Yu, Z.; Zhang, J.; Coulston, R. J.; Parker, R. M.; Biedermann, F.; Liu, X.; Scherman, O. A.; Abell, C. Supramolecular Hydrogel Microcapsules via Cucurbit[8]uril Host–guest Interactions with Triggered and UV-controlled Molecular Permeability. *Chem. Sci.* **2015**, *6*, 4929–4933.
- (5) Yin, S.-N.; Yang, S.; Wang, C.-F.; Chen, S. Magnetic-Directed Assembly from Janus Building Blocks to Multiplex Molecular-Analogue Photonic Crystal Structures. *J. Am. Chem. Soc.* **2016**, *138*, 566–573.
- (6) Yang, S.; Wang, C.-F.; Chen, S. Interface-Directed Assembly of One-Dimensional Ordered Architecture from Quantum Dots Guest and Polymer Host. *J. Am. Chem. Soc.* **2011**, *133*, 8412–8415.
- (7) Bai, S.; Debnath, S.; Gibson, K.; Schlicht, B.; Bayne, L.; Zagnoni, M.; Ulijn, R. V. Biocatalytic Self-Assembly of Nanostructured Peptide Microparticles using Droplet Microfluidics. *Small* **2014**, *10*, 285–293.
- (8) Baret, J.-C.; Miller, O. J.; Taly, V.; Ryckelynck, M.; El-Harrak, A.; Frenz, L.; Rick, C.; Samuels, M. L.; Hutchison, J. B.; Agresti, J. J.; Link, D. R.; Weitz, D. A.; Griffiths, A. D. Fluorescence-Activated Droplet Sorting (FADS): Efficient Microfluidic Cell Sorting Based on Enzymatic Activity. *Lab Chip* **2009**, *9*, 1850–1858.
- (9) Du, G.-S.; Pan, J.-Z.; Zhao, S.-P.; Zhu, Y.; den Toonder, J. M. J.; Fang, Q. Cell-Based Drug Combination Screening with a Microfluidic Droplet Array System. *Anal. Chem.* **2013**, *85*, 6740–6747.

- (10) Du, W.; Sun, M.; Gu, S.-Q.; Zhu, Y.; Fang, Q. Automated Microfluidic Screening Assay Platform Based on DropLab. *Anal. Chem.* **2010**, *82*, 9941–9947.
- (11) Joansson, H. N.; Andersson, H. Droplet Microfluidics—A Tool for Single-Cell Analysis. *Angew. Chem., Int. Ed.* **2012**, *51*, 12176–12192.
- (12) Kang, D.-K.; Ali, M. M.; Zhang, K.; Huang, S. S.; Peterson, E.; Digman, M. A.; Gratton, E.; Zhao, W. Rapid Detection of Single Bacteria in Unprocessed Blood Using Integrated Comprehensive Droplet Digital Detection. *Nat. Commun.* **2014**, *5*, 5427.
- (13) Schneider, T.; Kreutz, J.; Chiu, D. T. The Potential Impact of Droplet Microfluidics in Biology. *Anal. Chem.* **2013**, *85*, 3476–3482.
- (14) Chen, Z.; Liao, P.; Zhang, F.; Jiang, M.; Zhu, Y.; Huang, Y. Centrifugal Micro-channel Array Droplet Generation for Highly Parallel Digital PCR. *Lab Chip* **2017**, *17*, 235–240.
- (15) Jakiela, S.; Kaminski, T. S.; Cybulski, O.; Weibel, D. B.; Garstecki, P. Bacterial Growth and Adaptation in Microdroplet Chemostats. *Angew. Chem., Int. Ed.* **2013**, *52*, 8908–8911.
- (16) Koo, K. M.; Wee, E. J. H.; Wang, Y.; Trau, M. Enabling Miniaturised Personalised Diagnostics: from Lab-on-a-chip to Lab-in-a-drop. *Lab Chip* **2017**, *17*, 3200–3220.
- (17) Sukhanova, A.; Volkov, Y.; Rogach, A. L.; Baranov, A. V.; Susha, A. S.; Klinov, D.; Oleinikov, V.; Cohen, J. H. M.; Nabiev, I. Lab-in-a-drop: Controlled Self-assembly of CdSe/ZnS Quantum Dots and Quantum Rods into Polycrystalline Nanostructures with Desired Optical Properties. *Nanotechnology* **2007**, *18*, 18S602.
- (18) Anna, S. L.; Bontoux, N.; Stone, H. A. Formation of Dispersions Using “Flow Focusing” in Microchannels. *Appl. Phys. Lett.* **2003**, *82*, 364–366.
- (19) Nisisako, T.; Torii, T.; Takahashi, T.; Takizawa, Y. Synthesis of Monodisperse Bicolored Janus Particles with Electrical Anisotropy Using a Microfluidic Co-Flow System. *Adv. Mater.* **2006**, *18*, 1152–1156.
- (20) Chu, L.; Utada, A. S.; Shah, R. K.; Kim, J.-W.; Weitz, D. A. Controllable Monodisperse Multiple Emulsions. *Angew. Chem., Int. Ed.* **2007**, *46*, 8970–8974.
- (21) Zhang, L.; Feng, Q.; Wang, J.; Sun, J.; Shi, X.; Jiang, X. Microfluidic Synthesis of Rigid Nanovesicles for Hydrophilic Reagents Delivery. *Angew. Chem., Int. Ed.* **2015**, *54*, 3952–3956.
- (22) Thorsen, T.; Roberts, R. W.; Arnold, F. H.; Quake, S. R. Dynamic Pattern Formation in a Vesicle-Generating Microfluidic Device. *Phys. Rev. Lett.* **2001**, *86*, 4163–4166.
- (23) Song, H.; Tice, J. D.; Ismagilov, R. F. A Microfluidic System for Controlling Reaction Networks in Time. *Angew. Chem., Int. Ed.* **2003**, *42*, 768–772.
- (24) Cramer, C.; Fischer, P.; Windhab, E. J. Drop Formation in a Co-flowing Ambient Fluid. *Chem. Eng. Sci.* **2004**, *59*, 3045–3058.
- (25) Zhao, Y.; Gu, H.; Xie, Z.; Shum, H. C.; Wang, B.; Gu, Z. Bioinspired Multifunctional Janus Particles for Droplet Manipulation. *J. Am. Chem. Soc.* **2013**, *135*, 54–57.
- (26) Shang, L.; Cheng, Y.; Wang, J.; Ding, H.; Rong, F.; Zhao, Y.; Gu, Z. Double Emulsions from a Capillary Array Injection Microfluidic Device. *Lab Chip* **2014**, *14*, 3489–3493.
- (27) Gu, H.; Duits, M. H.; Mugele, F. Droplets Formation and Merging in Two-Phase Flow Microfluidics. *Int. J. Mol. Sci.* **2011**, *12*, 2572–2597.
- (28) Kaminski, T. S.; Scheler, O.; Garstecki, P. Droplet Microfluidics for Microbiology: Techniques, Applications and Challenges. *Lab Chip* **2016**, *16*, 2168–2187.
- (29) Duncombe, T. A.; Tentori, A. M.; Herr, A. E. Microfluidics: Reframing Biological Enquiry. *Nat. Rev. Mol. Cell Biol.* **2015**, *16*, 554–567.
- (30) Shang, L.; Cheng, Y.; Zhao, Y. Emerging Droplet Microfluidics. *Chem. Rev.* **2017**, *117*, 7964–9040.
- (31) Dendukuri, D.; Doyle, P. S. The Synthesis and Assembly of Polymeric Microparticles Using Microfluidics. *Adv. Mater.* **2009**, *21*, 4071–4086.
- (32) Datta, S. S.; Abbaspourrad, A.; Amstad, E.; Fan, J.; Kim, S.-H.; romanowsky, M.; Shum, H. C.; Sun, B.; Utada, A. S.; Windbergs, M.; Zhou, S.; Weitz, D. A. 25th Anniversary Article: Double Emulsion Templated Solid Microcapsules: Mechanics And Controlled Release. *Adv. Mater.* **2014**, *26*, 2205–2218.
- (33) Wu, P.; Wang, Y.; Luo, Z.; Li, Y.; Li, M.; He, L. A 3D Easily-assembled Micro-Cross for Droplet Generation. *Lab Chip* **2014**, *14*, 795–798.
- (34) Sun, K.; Wang, Z.; Jiang, X. Modular Microfluidics for Gradient Generation. *Lab Chip* **2008**, *8*, 1536–1543.
- (35) Zhang, K.; Gao, M.; Chong, Z.; Li, Y.; Han, X.; Chen, R.; Qin, L. Single-cell Isolation by a Modular Single-cell Pipette for RNA-sequencing. *Lab Chip* **2016**, *16*, 4742–4748.
- (36) Bhargava, K. C.; Thompson, B.; Malmstadt, N. Discrete Elements for 3D Microfluidics. *Proc. Natl. Acad. Sci. U. S. A.* **2014**, *111*, 15013–15018.
- (37) Bertsch, A.; Heimgartner, S.; Cousseau, P.; Renaud, P. Static Micromixers Based on Large-scale Industrial Mixer Geometry. *Lab Chip* **2001**, *1*, 56–60.
- (38) Xu, P.; Zheng, X.; Tao, Y.; Du, W. Cross-Interface Emulsification for Generating Size-Tunable Droplets. *Anal. Chem.* **2016**, *88*, 3171–3177.
- (39) Liao, S.; He, Y.; Wang, D.; Dong, L.; Du, W.; Wang, Y. Dynamic Interfacial Printing for Monodisperse Droplets and Polymeric Microparticles. *Adv. Mater. Technol.* **2016**, *1*, 1600021.
- (40) Hu, Y.; Xu, P.; Luo, J.; He, H.; Du, W. Absolute Quantification of H5-Subtype Avian Influenza Viruses Using Droplet Digital Loop-Mediated Isothermal Amplification. *Anal. Chem.* **2017**, *89*, 745–750.
- (41) Martin, M. M.; Lindqvist, L. The pH dependence of Fluorescein Fluorescence. *J. Lumin.* **1975**, *10*, 381–390.
- (42) Baraban, L.; Bertholle, F.; Salverda, M. L.; Bremond, N.; Panizza, P.; Baudry, J.; de Visser, J. A. G. M.; Bibette, J. Millifluidic Droplet Analyser for Microbiology. *Lab Chip* **2011**, *11*, 4057–4062.
- (43) Boedicker, J. Q.; Li, L.; Kline, T. R.; Ismagilov, R. F. Detecting Bacteria and Determining Their Susceptibility to Antibiotics by Stochastic Confinement in Nanoliter Droplets Using Plug-based Microfluidics. *Lab Chip* **2008**, *8*, 1265–1272.
- (44) Liu, P.; Li, P.; Jiang, X.; Bi, D.; Xie, Y.; Tai, C.; Deng, Z.; Rajakumar, K.; Ou, H.-Y. Complete Genome Sequence of *Klebsiella pneumoniae* subsp. *pneumoniae* HS11286, a Multidrug-Resistant Strain Isolated from Human Sputum. *J. Bacteriol.* **2012**, *194*, 1841–1842.
- (45) Clinical and Laboratory Standards Institute. Performance Standards for Antimicrobial Susceptibility Testing; Twenty-Fifth Informational Supplement; [www.clsi.org](http://www.clsi.org), 2015.